Simulation Study of Semi-Crystalline Polymer Interphases

S. Balijepalli and G. C. Rutledge*

Department of Chemical Engineering, Massachusetts Institute of Technology, Cambridge, MA 01239, U.S.A.

SUMMARY: The study of structure and properties of semi-crystalline polymer interphases is important to explain and extend polymer applications. In this region, polymer chains exist in three distinct populations: tie chains that bridge the two crystals, chain folds and chain ends. The distribution of these populations influences the properties of the interphase. We have developed off-lattice Monte Carlo simulations of constrained interphases of semi-crystalline polymers which utilize robust off-lattice moves. A united atom model with polyethylene-like interactions and with freely rotating bonds is used to mimic the prototypical flexible chain structure. These simulations capture the limiting distributions of tight and loose chain folds and of tie chains within the metastable phase. The dissipation in order and density between the crystal and amorphous regions has been studied, and results for freely rotating chains indicate that the characteristic decay of anisotropy occurs in a length scale of ca. 10 Å. Simulation results for the effect of system size and molecular weight for freely rotating chains have also been investigated.

1 Introduction

Semi-crystalline polymers in their solid state exhibit complex morphologies. The long chain nature of the constituent molecules, unique to polymers, has an extremely important influence on the structure. The predominant morphology consists of chains threading through alternating layers of crystalline and amorphous lamel-

 CCC 1022-1360/98/$ 17.50

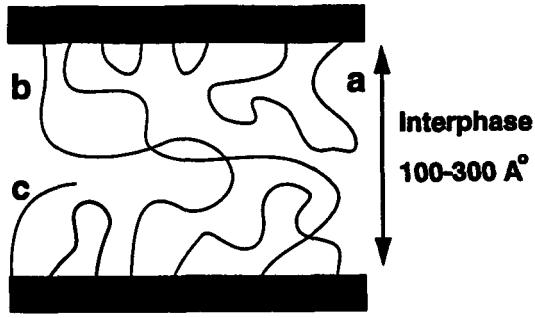

Figure 1: A sketch of the interphase region of semi-crystalline polymers. Three conformations of chains are shown: a) folds b) tie chains c) chain ends.

lar regions. The morphology and structure of these regions determines the overall performance of the polymer. An important step towards understanding the performance of a multiphase material is establishing quantitatively the relation between macroscopic properties and microscopic structure.

Figure 1 is a sketch of the non-crystalline region between two lamellar crystallites. The inter-lamellar region is typically 100-300 Å in semi-crystalline polymers like polyethylene (PE). The inter-lamellar region of semi-crystalline polymers has been the subject of extensive study[1-2]. Several experimental techniques, primarily, small-angle X-ray scattering[3-4], proton NMR[5-7], Raman spectroscopy[4,8,9], neutron scattering[10-11], and specific heat measurements[12] have been utilized. Scatter-

ing techniques are sensitive to the density distribution and spectroscopic techniques to the orientational distribution of polymer segments in the amorphous region. Comparative studies of the various techniques to quantify the inter-lamellar structure of PE have been reported in the past[3,13–14] and most recently by Stribeck *et al*[4]. As a result, it has been concluded that the interlamellar region could be divided into two zones, the first zone consisting of an interfacial region close to the crystal surface which is anisotropic and a second zone which is liquid-like in nature and truly amorphous. In this paper the term 'interphase' will be used to mean the complete region and 'interface' the anisotropic region close to the crystal surface. The interfacial region along with the crystal and liquid-like regions constitute a three component model for semi-crystalline polymers. The extent of the interfacial component, using PE's of different molecular weights and by different methods, is on the order of 8-10 Å in thickness and independent of molecular weight[3,4]. Some discrepancies do exist between the results of each of the methods, though the values are in the same order of magnitude. However, these experimental techniques do not provide us with a method for quantifying the properties of the interphase. For polymers, invariably, the data collected depend on the previous history of the sample. Molecular weight distributions and non-equilibrium crystallizing conditions result in a large distribution of crystal and amorphous zone sizes and therefore affect the spectra obtained. Furthermore, models with adjustable parameters are invoked to fit the experimental spectrum. This results in model-dependent properties.

Furthermore, while experimental techniques provide us with macroscopic measurements of the inter-lamellar region, they do not reveal the molecular structure associated with this region. The material in this region is in a metastable state

locked in by the constraints of the crystal faces. Polymer chains in this region are of three types: tie chains that bridge crystals, chain folds and chain ends. The flux of chains near the crystal surface is high and decreases in the middle region. In addition, there is a decay of the density from that of the crystal to that of the amorphous material in the middle region. This dissipation in the flux of chains is related to the conformation of chains in the interfacial region. If a portion of chains from the crystal surface fold back, they do not contribute to the flux in the liquid-like region. Chain conformations can be tightly folded or loosely folded; chain ends could be localized near the crystal surface or contribute to the liquid-like region. Clearly, the issue of dissipation of density and order associated with the interfacial region is related to the local structure which cannot be probed easily with experimental techniques. Atomistic modeling and simulations are ideal tools for tackling this problem. A molecular level study of chain conformations is necessary to understand the various issues related to the inter-lamellar zone and would be important to establish a three-component model of semi-crystalline polymers.

In the past, simulations and analytical techniques have been utilized to model polymer interphases. One analytical technique has treated conformations in the amorphous region as random walks with absorbing barriers[15~16]. Based on random walk statistics, if all chains from the crystal phase contribute to the liquid-like region, the density of the region would be three times that of the crystal phase. To explain this discrepancy, it was proposed that the flux is reduced because two-thirds of the chains fold back without contributing to the liquid-like region. However, these models do not tell us anything about the extent of the interfacial zone. Lattice models have been developed to study the extent of the interfacial zone. These are based

on Monte Carlo[17-18] methods and mean-field approaches[19-21]. According to these models the decay of orientational ordering occurs in 2-5 lattice layers depending on the bending energy associated with folded chains. Furthermore, the degree of tight folding (as defined by chains which connect adjacent sites on the crystal faces) obtained is 72% for fully flexible lattice chains and decreases to about 30% for stiffer chains. However, lattice models are limited in their representation of the interphase. Though they capture the decay of orientational ordering, they do not account for the decrease in density. Obviously, both these aspects taken together influence the state of the material. The decay of order arises from entropic forces whereas the decay of density depends on packing considerations. An interplay of entropic and energetic forces determines the metastable state of the interphase.

Unlike these lattice models, atomistic models incorporate realistic effects of chain architecture and geometry along with realistic potentials of interaction. Atomistic detail conferred on a model uses the right combination of entropic and energetic factors to simulate real interphases. Such simulations also does not presuppose any previous history of the polymer and a great degree of control can be exercised in defining the state of the material. Quantitative properties can be obtained. For semi-crystalline polymers, thermal, mechanical and thermodynamic properties are dependent on the interphase. As an example, anisotropic interphases with large numbers of tie chain conformations would result in a tougher material, resistant to deformation. An off-lattice simulation study provides a direct way of obtaining quantitative properties that would go towards building a better constitutive model for semi-crystalline polymers.

In this article, we present the results of the first off-lattice simulations, using Monte Carlo techniques, of the interphase of semi-crystalline polymers. The simulation of the interphase was implemented using robust off-lattice Monte Carlo (MC) moves which utilize cutting and splicing of chains with Metropolis sampling. In the process, atomistically detailed structures of a constrained equilibrium state are generated which represent the amorphous zone of the polymer sandwiched between crystallites. By construction of the simulation, we have generated metastable phases and studied their structural aspects. Monte Carlo algorithms utilized in this study have been developed for simulations of dense phases of amorphous polymers[22-23] and are adapted here to simulate dense interphases.

Simulation results of interphases of freely rotating chains are presented in the paper. The paper is organized as follows : the model is presented in section 2, the simulation details are presented in section 3, results are described in section 4 and summary and discussion are provided in section 5.

2 The Model

In simulations reported here the polymer chain consists of methylene units modeled as united atoms connected to each other by fixed bond lengths of 1.53 Å and the supplements of the carbon-carbon-carbon bond angles are fixed at 68^o. Torsions about each bond are allowed to rotate freely. All interactions, inter-chain and intra-chain, for pairs of united atoms are modeled with the same non-bonded potential. A Lennard-Jones (LJ) form with parameters $\sigma = 3.94$ Å and $\epsilon/k = 49.3$ K is utilized. For MC simulation of the interphase, the LJ potential was modified for

a finite range of interaction (shifted force potential[25]) and the potential was set to zero beyond the cutoff radius, defined as $\min(2.5\sigma, L_{min}/2)$, where L_{min} is the minimum length of one of the sides of the simulation cell.

The interphase is modeled as an orthorhombic box with the bottom and top (z=0,L_z) faces corresponding to the < 001 > faces of the crystallites. Typical dimensions in the x and y directions are 22.2Å and 14.7Å respectively and correspond to three unit cells in each of the directions. Polymer chains from each of the crystal sites contribute to the interphase. The thickness L_z of the interphase is varied in this study. Periodic boundary conditions are employed in the x and y directions and permit the treatment of the system macroscopically in the two lateral directions. To model the crystalline boundary, the first three sites on a chain at the top and bottom crystal faces are fixed at their crystallographic positions. This design of the boundary ensures the continuity of angular constraints as chains emerge from the crystal phase into the interphase.

3 Details of Simulation

The aim of the simulation is to capture the detailed structure of the interphase. Chains emerging from the crystal phases should be in crystallographic order and this is modeled by keeping the first three sites of a chain at the top and bottom faces in crystallographic registry. Secondly, the average interphase density is lower than the crystal phase density. The generation of an initial structure satisfying this requirement was accomplished by reducing the number density of atoms in the simulation cell. Initially, a crystal phase of the simulation cell was constructed with

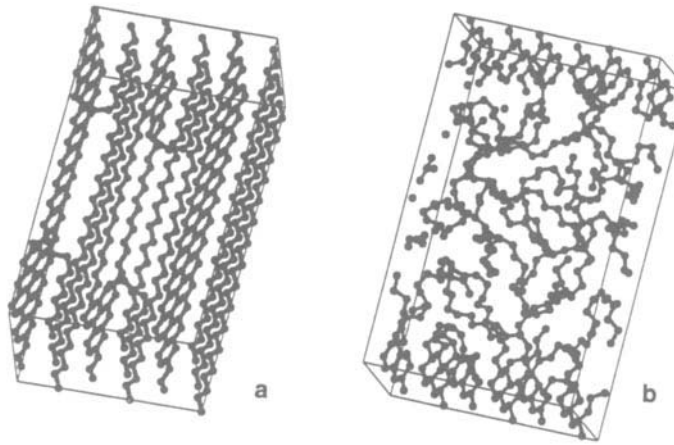

Figure 2: Generation of initial structure : a) a hole is made in the cell b) cutting and splicing of chains used to generate an amorphous structure.

all chains in the all *trans* configuration bridging crystal sites of the two crystal faces. Atoms in the cell were then removed in two ways. In the first method, adjacent chains were identified and, using the cutting and splicing algorithms to be described later, the two chains were joined to form two folded chains with the simultaneous removal of atoms. This creates a hole in the crystal phase (see also Figure 2) of the simulation cell. In the second method, chains that bridge the crystal phases were cut and atoms removed. This introduces chain ends into the simulation cell.

The removal of atoms is important in two ways. The creation of a hole in the crystal phase results in the system being driven away from its natural equilibrium

crystalline state. Due to the hole created, there aren't enough atoms to bridge the two crystal faces in the all *trans* crystal configuration. This results in a 'frustrated' system. By construction, the crystal phase boundaries are modeled as fixed. This, coupled with the crystal phase instability in the interphase, drives the atoms in the cell to a metastable configuration naturally during the course of the simulation.

In the second step of the initial structure generation, the chains in the simulation cell are cut and spliced using only a hard sphere potential (overlap $=0.8\sigma$) to accept or reject configurations. The configurations are sampled uniformly and hence randomly. This generates a liquid-like state consistent with the excluded volume criteria. However, the non-bonded interaction energies are high, and in the next stage of generation the interaction potentials are turned on to minimize the energy of the interphase. The Metropolis criterion is used in the selection of configurations. This results in a structure free of excessive atom-atom overlap and low intra- and inter- molecular energies with a distribution of chain populations and conformations. The initial structure generated in this fashion is equilibrated and, in the final run, collection undertaken to obtain the ensemble-averaged properties of the interphase. Details of equilibration criteria and relaxation characteristics of interphase systems are reviewed elsewhere[25].

An alternate method of construction of the initial structure has been done in the past by Brown and Clarke[26]. In that work, atoms in the interphase are initially grown starting from the crystal faces in a site-by-site manner. If two sites on different chains approach within a "capture radius", equal to the bond length, during the initial structure generation step, the sites are joined together to form permanent

bridges which can either be tie chains or folds; otherwise, they are left as chain ends. The method results in a large number of chain ends and a small number of chain folds. In Ref.26, the interphase generated in this manner was subsequently relaxed by molecular dynamics (MD). Our method of construction allows the number of chain ends to be fixed, while the MC method employed generates the proper limiting equilibrium distribution of tie and fold chain populations.

3.1 Monte Carlo Moves

To sample structure fluctuations in the interphase region, several MC methods have been utilized in this work. An important difference between the simulation of a thermodynamic equilibrium phase and the metastable interphase is that the terminus of each chain segment is fixed to the crystal surface. This constraint results in the inapplicability of reptation moves[27-28] that have been successfully used to relax dense single phases. Local moves are based on the Concerted Rotation (CR) algorithm developed by Dodd, Boone and Theodorou[22] which allow relaxation of chain configurations independent of chain ends.

The CR algorithm is based on a geometric solution which was first developed by McMohan *et al*[29] to study defects in polymer crystals and was later utilized by Gō and Scheraga[30] to study conformational relaxations in linear and cyclic molecules. The algorithm was successfully integrated into an MC scheme and is now a powerful method for efficient local relaxation of polymer chains[22]. The MC scheme requires the removal of four atoms bridging two sites in the forward move and rebridging in the backward move while satisfying the constraints of distance and orientation of the

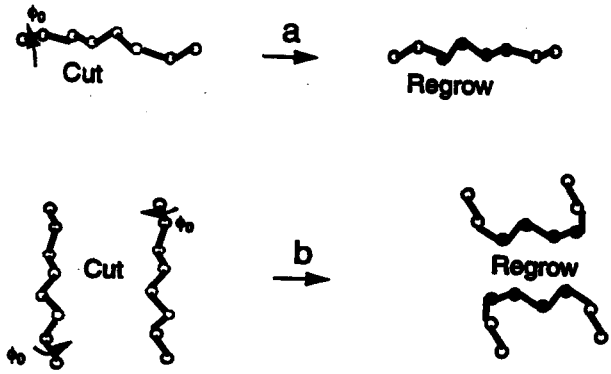

Figure 3: Forward moves of: a) Intra-chain Concerted Rotation b) Inter-chain Concerted Rotation.

sites. Microscopic reversibility is ensured by taking care to evaluate all solutions of the geometric problem and the inclusion of Jacobians of coordinate transformations into the MC scheme. Three moves are utilized based on the algorithm and are shown in Fig. 3. The first of these is the standard algorithm and is called the intra-chain CR move. A variant has been developed in this work to apply the move to cutting and splicing of two chains and is called the inter-chain CR move and is independent of chain ends. This move has been utilized in the generation of the initial structure with minimum overlap criteria. It was found to be relatively inefficient when full potentials of interaction were included. The interphase structure is allowed to relax by another variant of the two chain move which is dependent on the presence of chain ends. This move was developed by Pant and Theodorou[23] as

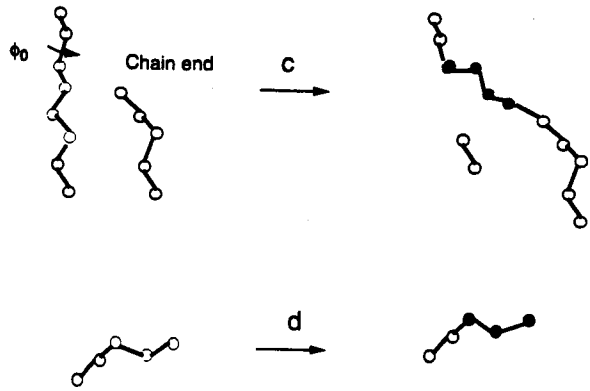

Figure 4: Forward moves for chain ends: c) end-bridging d) end rotation.

the end-bridging algorithm. Finally, the relaxation of chain ends is also accomplished by end-rotations. A sketch of the moves involving chain ends is shown in Fig.4. The intra-chain CR move allows local relaxation internal to the polymer chain and is analogous to short time relaxations, whereas the inter-chain CR and the end-bridging moves change the polymer connectivity and hence the end-to-end vector of the chain, allowing long-range relaxation of conformations. In the process, chain folds, tie chains and chain ends of different length are sampled. In our simulations, all chain lengths with 6 beads or more were allowed.

In the implementation of moves based on the CR algorithm, a screening procedure was employed to cull out viable solutions obtained by solving the geometric problem of bridging. All solutions satisfying a hard sphere overlap criteria (0.8σ)

were selected. This was done uniformly for the backward and forward moves. The attempt probabilities of the forward and reverse moves for freely rotating chains are given by,

$$\alpha(m \rightarrow n) = 1/N_n, \quad \alpha(n \rightarrow m) = 1/N_m \tag{1}$$

where, N_n and N_m are the forward and backward solutions in the CR algorithm after screening.

Special care was taken in the implementation of the inter-chain CR and end-bridging moves to ensure the proper probabilities of site selection. A site on a chain is selected to bridge to a second site selected on another chain. The probability of selecting this site depends on the number of non-bonded neighbors. Neighbor lists are updated in the forward and backward moves and included into the Metropolis criteria for the acceptance of the move given by,

$$P(m \rightarrow n) = min\left[1, \frac{(1/N_{nb}(m))\alpha(n \rightarrow m)exp(-V(n)/kT)J(n)}{(1/N_{nb}(n))\alpha(m \rightarrow n)exp(-V(m)/kT)J(m)}\right] \tag{2}$$

where $N_{nb}(m)$ and $N_{nb}(n)$ are the number of non-bonded neighbors, $J(m)$ and $J(n)$ are the Jacobians of transformation, $V(m)$ and $V(n)$ are the potential energies of the conformations in the backward and forward moves. Rotation of chain ends were accepted with probability,

$$P(m \rightarrow n) = min\left[1, \frac{exp(-V(n)/kT)}{exp(-V(m)/kT)}\right] \tag{3}$$

For the purpose of energy calculations, the interaction of the atoms in the interphase with those of the crystal phase were taken into account by considering

all crystal neighbors within a radius of cutoff of 7.35 Å ($L_y/2$) in the forward and backward moves.

3.2 Systems Studied

Monte Carlo simulations were carried out for freely rotating chains of PE. The first system studied consisted of a total of 23 chains at an average density of 0.88 gm/cc and had ten chain ends (denoted as I)[1]. The z dimensions of the box were 45.4 $\mathring{A}$ and correspond to $N_{bridge} = 36$ where N_{bridge} is the number of atoms required to bridge the two crystal faces in an all *trans* configuration. A second system was studied and had 19 chains at an average density of 0.91 gm/cc and two chain ends (denoted as II) with $N_{bridge} = 30$. The number of chains and the number of chain ends is conserved in the simulation. The effect of decreasing the number of chain ends is to increase the effective molecular weight of the material being simulated in the interphase zone. At the limit of zero chain ends, the molecular weight of the material becomes infinite.

4 Results

Results for systems I and II are presented in this section. The simulations provide us with a detailed picture of the structure of the interphase at the level of chain conformations. Results of an equilibrated run for system I, at 450 K are

[1]The total number of chains is the number of chains entering the interphase at the crystal boundaries (i.e. 36 for two 3×3 arrays of PE unit cells) plus the number of chain ends, divided by two

presented first. The Monte Carlo moves during this simulation were intra-chain CR, end-bridging and end rotations attempted in the ratio 35:105:3. During the collection run, a total of 5000 configurations were stored from which properties were determined as the ensemble average over the configurations. The simulation cell was divided into layers in the z-direction. The first and the last layers were 2.54 Å in size and correspond to the three fixed sites that are in crystallographic registry. The intermediate layers were 1.27 Å thick. Since the simulations were symmetric about the midplane of the simulation cell, accumulation of properties in each layer were superposed with its mirror image across the midplane. This reduces the statistical uncertainty. All the structural features presented are symmetrized plots with $z = 0$ corresponding to the crystal phase.

Density Distribution

The first property studied was the density distribution of the interphase. The density distribution along the z-axis is shown in Fig. 5. The density represents the ratio of the number density in the slice to the number density of the crystal phase. Two zones can be clearly distinguished in the figure, an interfacial region of roughly 10 Å where the density oscillates, and a region where the density fluctuations are dampened out to a bulk value. The oscillations in density have been observed previously in simulations of polymer chains interacting with a hard wall[31], where they are a result of a layering phenomena associated with packing atoms. However, the density oscillations in our simulations can be attributed to the nature of chain conformations in the interfacial region. Folding of chains results in an increased number of atoms in the fold plane resulting in an increase in density. This is reflected in

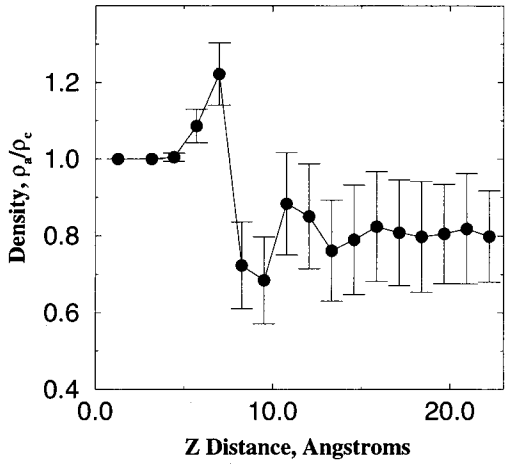

Figure 5: Density profile for system I, at 450 K, average density of 0.88 gm/cc and 10 chain ends in the simulation cell.

the region 5-8 Å from the crystal surface. Once the fold plane is crossed, there is a decrease in density of the interface which is substantiated by the rapid dampening of oscillations observed between 8 and 12 Å from the crystal surface. The amorphous density predicted in the liquid-like regions is 0.8 gm/cc and is lower than the experimental values of 0.85 gm/cc reported for low molecular weight PE[3]. However, it must be pointed out that reported experimental values are based on a two phase model. Recall that the first three sites on the top and bottom faces were taken to be in crystallographic order, and our initial average density of 0.88 gm/cc included

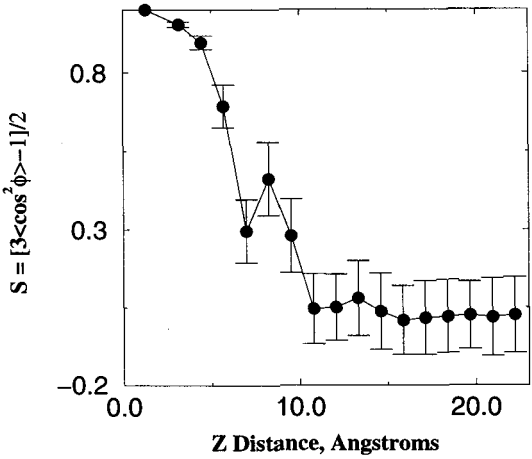

Figure 6: Order profile for system I, at 450 K, average density of 0.88 gm/cc and 10 chain ends in the simulation cell.

these sites. By construction, the average density of the cell disregarding these sites is in fact 0.84 gm/cc, closer to experimental amorphous densities.

Bond Orientation Distribution

Another important way to characterize the interphase is to study the bond orientation order parameter defined as,

$$S = [3 < cos^2\phi > -1]/2 \tag{4}$$

where ϕ is the angle measured by the $C-C-C$ bond chord with respect to the z-plane, and $< >$ represents the average over all configurations within the layer. S takes on values 0, 1 and -1/2 when the bond chords are randomly oriented, in crystallographic registry or parallel to the surface plane, respectively. The results of our study are shown in Fig. 6. This represents a decrease in order from the crystal surface into the bulk. As in the case of the density profile, two regions can be distinguished, an interfacial region with loss of orientation of the chains and a liquid-like region where the orientations are random. The bond orientation parameter decreases corresponding to an increase in density of the fold plane. The decrease in order occurs along a distance of 10 Å. The bond orientation parameter along with the density profile are sufficient to characterize the region as amorphous.

The torsional state of chains were also studied. Due to the constraints of fixed crystal surfaces and chain connectivity between the interphase and the crystals, the chain torsional states are expected to be different. To quantify this effect, we have divided the torsional space into 20 bins of 18^o each. Within each z-slice, rotation angles were assigned to the appropriate interval. The midpoint of the bond position was utilized to assign the angle to the layers along the z direction. In Fig. 7, the torsional distribution at three z positions is shown. Near the crystal surface (z=3.2 Å), the *trans* configuration is predominant. In the interface region (z=8 Å) there is only a slight residual of *trans* configurations. The torsional distributions for higher z values (corresponding to the amorphous region) are identical to the distribution at z=8 Å.

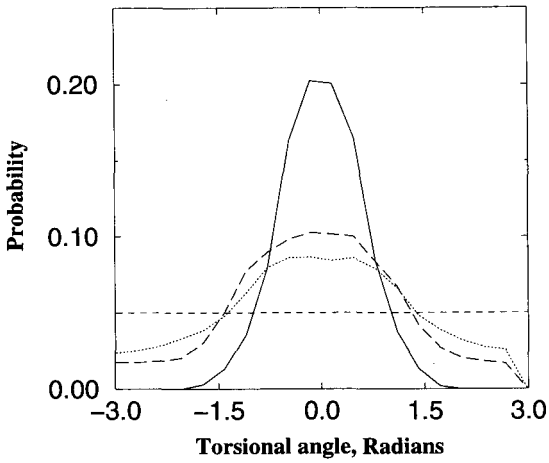

Figure 7: Torsional distribution of chains in the cell, at 450 K, 0.88 gm/cc and 10 chain ends in the simulation cell. Solid line at z= 3.2 Å. Long dashed line at z= 6.0 Å. Dotted line, z = 8.0 Å. Horizontal dashed line, represents uniform probability.

Chain Population Distribution

A third important property studied was the distribution of chain populations in the interphase. Three populations, namely folded chains, ties and chain ends are present in the interphase. Of these, the number of chain ends is kept fixed. Folds and ties of differing length are generated by the end-bridging algorithm. As an aside, we note that the changes in lengths of chains brought about by these moves does not imply any change in the molecular weight or polydispersity of the material

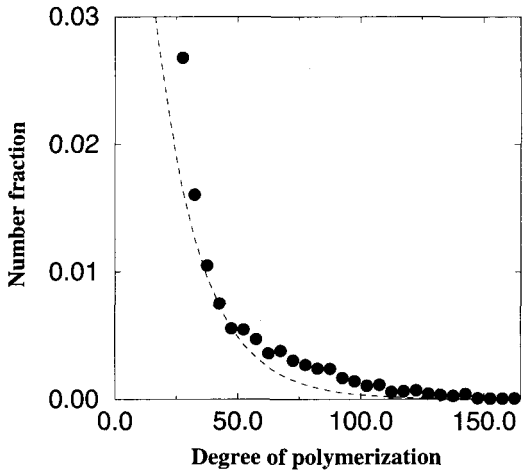

Figure 8: Chain length distribution for folds and tie chains. Dashed curve is the theoretical curve given by eqn.(5). Filled circles, are results of simulation for system I, at 450 K, 0.88 gm/cc and 10 chain ends in the simulation cell.

being studied. This is fixed by the number of chain ends. Recall that all chain lengths with 6 or more beads were allowed. However, each of the chain populations has its own minimum allowed length. For tie chains, the minimum allowed length is clearly the number of atoms bridging the crystal faces in an all *trans* configuration. For the fold population the minimum length is dictated by the CR move involving a chain end and a fold. The minimum number of atoms required in the fold to satisfy micro-reversibility is 13, given that 4 atoms are to be regrown in an end-bridging move. Figure 8 is the distribution reflected in the combined populations of folds and

tie chains obtained in our simulations. Also plotted in Fig. 8 is the most probable distribution assuming that local energetics have no influence on the chain length distribution[23],

$$P(l) = \frac{1}{(X - k_{min} - 1)} \left[\frac{X - k_{min}}{X - k_{min} + 1}\right]^{(k-k_{min})}, \; k_{min} = 6 \qquad (5)$$

where $X = n/N$ is the average chain length, n is the total number of atoms in the box and N the total number of chains, both of which are conserved in the simulation. Above $X = 13$ the distribution in length for chain ends is similar to the distribution of tie chains and folds. For freely rotating chains, the predominant configurations are tight folds that do not contribute to the flux of chains into the amorphous region.

System	N_{bridge}	% F	% AE	% TAE
I	36	96.5	55	52
II	30	88.5	53	49
Ia	30	94.7	56	54
Ib	26	91.6	58	55

Table 1 : Distribution of folds and tie chains. F: folds, AE: adjacent entry folds (defined by the end-to-end distance $\leq$5 Å), TAE: tight adjacent entry folds (defined by less than 18 beads in a fold and end-to-end distance within 5 Å).

Table 1 (system I), also compares the population of tie chains and folded chains. The numbers are calculated as a percentage of the total tie and folded chains. Chain

ends are not included. Among the folded configurations, an "adjacent entry" fold is defined by crystal re-entry points being within 5 Å. Adjacent folds are further divided into "tight adjacent entry" folds (those with less than 18 beads in the chain) and "loose adjacent entry folds" (those with 18 or more beads in the chain). For freely rotating chains a large percentage of folds are formed, with the predominance of tight adjacent folds. Other results for the effect of the system size and molecular weight are also included in the table for comparison and will be discussed in the following sections.

System Size Convergence

The study of system size effects is necessary in many respects. The goal of our simulation is to capture the dissipation of anisotropy within the interfacial region. The interphase thickness has to be chosen large enough to make the middle region truly amorphous, yet small enough to make the simulation computationally tractable. Secondly, the fraction of chain conformations existing as tie chains depends on the separation between the crystal faces. If the polymer chains are modeled as a random walk between absorbing barriers the fraction of tie chains goes to zero asymptotically as the distance between crystals increases. Both aspects were studied. In Figs. 9 and 10, the two structural parameters of density and order are shown for three simulation sizes ($N_{bridge} = 26, 30, 36$, $L_z = 1.26 N_{bridge}$). All simulations studied for the effect of system size were at a temperature of 450 K, above the melting temperature of the freely rotating chain. However by construction, the crystal faces are fixed and only the middle region 'melts'. For $N_{bridge} = 26$, the density oscillations are large and persist throughout the interphase. The effect of the crystal

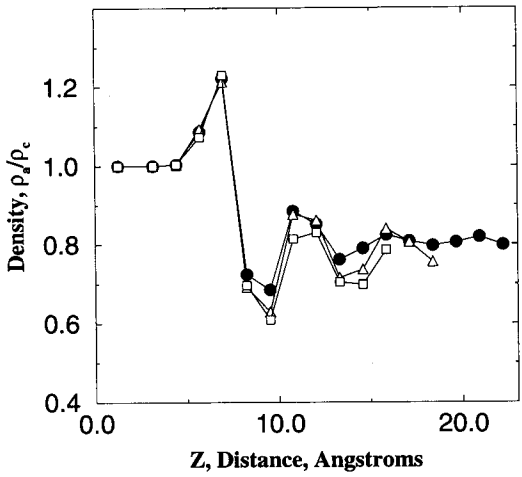

Figure 9: Density profile for three cell sizes. Filled circle is for a cell size N_{bridge}=36. Open triangles are for N_{bridge}=30 and open squares are for N_{bridge} = 26. All simulations were at 450 K and an average density of 0.88 gm/cc and 10 chain ends in the cell.

faces extends into the middle region, though the order parameter has reached the amorphous value. The distribution of chain conformations for the simulations are summarized in Table 1 (systems I, Ia and Ib, corresponding to $N_{bridge} = 36, 30, 26$ respectively). The percentage of tie chains decreases as L_z is increased, consistent with random walk statistics. The number of tie chains approaches zero asymptotically and our choice of $N_{bridge} = 36$ for the largest simulation cell size in the z direction results in a small fraction of tie chains.

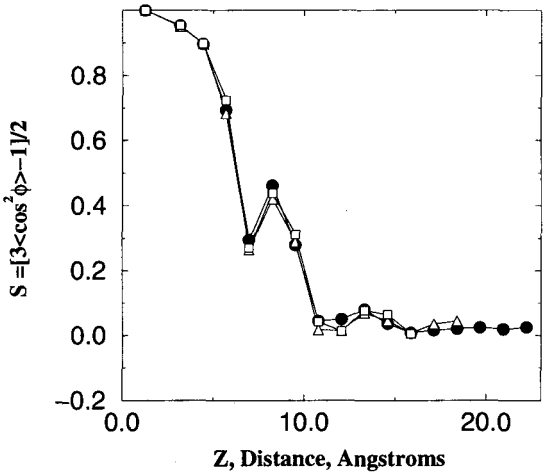

Figure 10: Order profile for three cell sizes. Filled circles are for a cell size N_{bridge}=36. Open triangles are for N_{bridge}=30 and open squares are for N_{bridge} = 26. All simulations were at 450 K and an average density of 0.88 gm/cc and 10 chain ends in the cell.

A second important size effect in the simulation study concerns the effective molecular weight of the material being studied. During crystallization of polymers, chain ends are partially or wholly excluded from the crystal lattice and occupy sites in the interphase region. Considerable evidence exists for this behavior and this aspect has been studied by X-ray scattering techniques[32]. The fraction of chain ends in the interphase is thus indicative of the molecular weight, which increases as the fraction of chain ends is decreased. An approximate analysis[25] suggests that

the effective molecular weight for system I with ten chain ends corresponds to $\approx$ $8000\,g/mol$. Reducing the number of chain ends to two results in a molecular weight around 30,000 g/mol. For a 450 K simulation with 2 chain ends and $N_{bridge} = 30$ (system II), the percentage of tie chains increases (refer to Table 1), but the extent of the interfacial region was found to be similar to that of the low molecular weight polymer (≈ 10Å).

5 Summary and Discussion

In summary, a realistic off-lattice model of semi-crystalline polymer interphases has been developed for the first time. Monte Carlo moves which alter both conformation and connectivity have been used to study the detailed structural features of the region. Simulations were performed using a united atom model with realistic potentials of interaction between non-bonded atom sites. Examination of local structural features shows that there is a decay of density and orientational order within a distance of 10 Å from the crystal surface. Limiting distributions of chain populations have been obtained. It was found that for freely rotating chains, tightly folded conformations of chains are preferred in the interfacial region. The effect of system size on the decay of anisotropy has been studied. A simulation cell of $z = 45.4$ Å was found to be adequate to allow oscillations in density and orientation to decay to values characteristic of the amorphous melt. The extent of the interfacial zone was found to be relatively insensitive to molecular weight below 30,000 g/mol. However, the fraction of tie chains was found to increase with molecular weight for a given interphase thickness.

The extent of the interfacial zone predicted is within the range of experimental observations (ca. 10 Å). In addition, the simulations capture the details of the local structure. The fraction of tight folds was found to be large, resulting in a fold plane with associated oscillations of density as seen in Fig.5. In Fig. 6 and 7, near the crystal surface, the density and order remain close to the crystal values as seen by the first three points. Subsequently, the order and density show rapid changes associated with the folding of chains. It can be construed that to a distance of 5 Å, the chains are extended with little lateral disorder and subsequently order is completely disrupted by folding. The extent of the interfacial zone predicted by these simulations is expected to be a lower bound value. With inclusion of more realistic torsion potentials, we expect an increase in size of the interfacial zone. The effect of molecular weight on the extent of the zone was found to be minimal for freely rotating chains. The distribution of chain populations for the case of 10 chain ends and 2 chain ends (Table 1), shows the predominance of folding. As the system size in the z-direction is increased, the percentage of folds increases relative to tie chain conformations. In addition, the degree of adjacent folds (as defined by the end points being adjacent to each other on the crystal lattice) decreases. Clearly, in this case, more loosely folded conformations contribute to the liquid-like amorphous zone and these results are in agreement qualitatively with lattice simulations of Mansfield[17].

The present model for freely rotating chains captures all the features of metastable interphases. By keeping the crystal phases fixed at the boundaries and decreasing the number density of the interphase by removing atoms, we have created a 'frustrated' system. The simulations generate limiting distributions of chain populations

and for freely rotating chains the predominant population is folds. Folded structures in the interphase zone represent the response of the material to the condition of metastability brought about by the constraints of connectivity and immobility at the crystal boundaries, combined with the temperature and density of the amorphous phase. As there is no energy penalty associated with bending chains in the freely rotating chain, we get a high percentage of folds. The formation of folded structures for freely rotating chains is because they are entropically preferred. However, folds disrupt packing and are not favored energetically. A balance of the two forces determines the chain populations. Within the fold population, the percentage of tight folds with their ends adjacent to each other is high. In addition, by forming tight folds, the interface is localized and a greater part of configurational space is available to the bulk of the interphase, which is truly amorphous and liquid-like. In Fig. 5 and Fig. 6, there are two zones associated with the interphase and both structural quantities show discontinuities between the zones. The simulation results can be interpreted as an attempt at phase separation in the simulation cell, with the interface consisting of the tightly folded material and the middle region consisting of liquid-like material.

Acknowledgments

This work was supported by NSF/MRSEC, through the Center for Material Science and Engineering at M.I.T, Grant number 9400334. We are also grateful to L. R. Dodd and D. N. Theodorou for their code of the Concerted Rotation algorithm[22].

References

[1] L. Mandelkern, *Acc. Chem. Res.*, **23**, 380, (1990)

[2] L. Mandelkern, *Chemtracts: Macromol.Chem.*, **3**, 347, (1992)

[3] G. R. Strobl, M. Schneider, *J. Polym. Sci., Polym. Phys. Ed.*, **18**, 1343, (1980)

[4] N. Stribeck, R. G. Alamo, L. Mandelkern, H. G. Zachmann, *Macromolecules*, **28**, 5029, (1995)

[5] R. R. Eckman, P. M. Henrichs, A. J. Peacock, *Macromolecules*, **30**, 2474, (1997)

[6] R. Kitamaru, T. Nakaoki, R. G. Alamo, L. Mandelkern, *Macromolecules*, **29**, 6847 (1996)

[7] R. Kitamaru, F. Horii, K. Murayama, *Macromolecules* , **19**, 636, (1986)

[8] G. R. Strobl, W. Hagedon, *J. Polym. Sci., Polym. Phys. Ed.*, **16**, 1181 (1978)

[9] C. C. Naylor, R. J. Meier, B. J. Kip, K. P. J. Williams, S. M. Mason, N. Conroy, D. L. Gerrard, *Macromolecules*, **28**, 2969 (1995)

[10] B. Crist, J. C. Nicholson, *Polymer*, **35**, 1846 (1994)

[11] E. W. Fischer, E. W. *Polymer*, **17**, 307, (1985)

[12] I. G. Voigt-Martin, G. M. Stack, A. J. Peacock, L. Mandelkern, *J. Polym. Sci., Polym. Phys. Ed.*, **27**, 957, (1989)

[13] I. G. Voigt-Martin, L. Mandelkern, *J. Polym. Sci., Polym. Phys. Ed.*, **16**, 987, (1989)

[14] S. Z. D. Cheng, B. Wunderlich, *Macromolecules*, **21**, 789, (1988)

[15] E. A. DiMarzio, C. M. Guttman, *Polymer*, **13**, 733, (1980)

[16] C. M. Guttman, E. A. DiMarzio, *Macromolecules*, **15**, 525, (1982)

[17] M. L. Mansfield, *Macromolecules*, **16**, 914, (1983)

[18] I. Zùñiga, K. Rodrigues, W. L.Mattice, *Macromolecules*, **23**, 4108, (1990)

[19] P. J. Flory, D. Y. Yoon, K. A. Dill, *Macromolecules*, **17**, 862, (1984)

[20] S. K. Kumar, D. Y. Yoon, *Macromolecules*, **22**, 3458, (1989)

[21] J. A. Marqusee, *Macromolecules*, **22**, 472, (1989)

[22] L. R. Dodd, T. D. Boone, D. N. Theodorou, *Mol. Phys.*, **78**, 961, (1993)

[23] K. V. Pant, D. N. Theodorou, *Macromolecules*, **28**, 7224, (1995)

[24] M. P. Allen, D. J. Tildesley *Computer Simulations of Liquids*, Oxford (1987)

[25] S. Balijepalli, G. C. Rutledge, manuscript in preparation

[26] D. Brown, J. H. R. Clarke, *J. Chem. Phys.*, **84**, 2858, (1986)

[27] M. Vacatello, G. Avitabile, P. Corradini, A. Tuzi, *J. Chem. Phys.*, **73**, 548, (1980)

[28] R. H. Boyd, *Macromolecules*, **22**, 2477, (1989)

[29] P. E. McMohan, R. L. McCullough, A. A. Schlegel, *J. Appl. Phys.*, **38**, 4123, (1967)

[30] N. Gō, H. A. Scheraga, *Macromolecules*, **3**, 178, (1970)

[31] J. Baschnagel, K. Binder, *Macromol. Theory Simul.*, **5**, 417, (1996)

[32] S. Balijepalli, J. M. Schultz, *Macromolecules*, **29**, 6601, (1996)